Available online at www.sciencedirect.com
ScienceDirect
Journal of Photochemistry and Photobiology A: Chemistry 189 (2007) 7–14
Journal of Photochemistry and Photobiology A:Chemistry
www.elsevier.com/locate/jphotochem

Preparation and optical properties of organic nanoparticles of porphyrin without self-aggregation

Zhong-min Ou, Hiroshi Yao *, Keisaku Kimura

Graduate School of Material Science, University of Hyogo, 3-2-1 Koto, Kamigori-cho, Ako-gun, Hyogo 678-1297, Japan

Received 25 July 2006; received in revised form 4 December 2006; accepted 30 December 2006
Available online 4 January 2007

Abstract

We report the synthesis and optical properties of organic porphyrin nanoparticles with narrow size distribution and well dispersibility. Ion association between cationic *meso*-tetrakis(1-methylpyridinium-4-yl) porphine (TMPyP) and tetraphenylborate (TPB) anion or fluorinated derivatives of TPB, in the presence of polyvinylpyrrolidone (PVP), produces the porphyrin nanoparticles of ~25 nm in aqueous solution. The TMPyP nanoparticles were stable in solution without precipitation for at least 30 days. No self-aggregation of the constituent porphyrin chromophores was confirmed. The TMPyP nanoparticles exhibited interesting optical properties; a large bathochromic shift in the absorption spectra and a resolution increase in the fluorescence spectra compared to those for the solution-phase TMPyP. A flattening of TMPyP molecules within the nanoparticles, which is caused by the twisting of four cationic methylpyridinium moieties, is the main origin for the large red shift. The resolution increase of fluorescence is due to the effect of immobilization of the methylpyridinium groups in the solid-state nanoparticles and/or that of a low polarity environment.

Keywords: Porphyrin nanoparticles; Ion association; Optical properties; Porphyrin flattening

1. Introduction

The successful development of molecular devices for applications in photochemical energy conversion and storage requires fundamental research of photofunctional organic materials [1]. Recent research also entails investigations of non-covalent organic assemblies or aggregates on nanometer scales because their optical properties significantly differ from those of monomeric species [2,3]. Porphyrins are representative of photofunctional organics, and they show remarkable photo-, electro- and biochemical properties that contributes to light harvesting by their strong absorption in photosynthesis [2]. Hence, the architectures of meso/nano-scaled porphyrin assemblies or particles are expected to be promising candidates for use in photonic devices [3].

Among the porphyrin compounds, photo-physical/chemical properties and aggregation behaviors of water-soluble *meso*-tetrakis(1-methylpyridinium-4-yl) porphine (TMPyP) have been so far well investigated [4,5]. In particular, the electrostatic interaction between the cationic TMPyP and anionic compounds has been widely focused via the studies on TMPyP–DNA, TMPyP–surfactant or TMPyP–clay complexes [6,7]. A more recent study involves nanotube formation by ionic self-assembly of two oppositely charged porphyrins [7]. Although it is undoubtedly important to design such nanoscale systems with ordered porphyrin assemblies, unfavorable aggregation that causes a large decrease in the color quality and/or photoluminescence should be avoided in the assemblies [8].

To fabricate organic nano-architectures composed of porphyrins, it should be recognized that van der Waals intermolecular and hydrogen-bonding interactions as well as the electrostatic attraction are responsible for the specific electronic/optical properties that are fundamentally different from those of inorganic metals or semiconductors [9]. In this article, we report the synthesis of organic nanoparticles of porphyrin by the "ion-association technique" that has advantages in simplicity and versatility [10]. The method is based on the formation of water-insoluble ion-pair-based nanoparticles in aqueous solution by the association of a dye cation with a hydrophobic anion. TMPyP is selected as a cationic porphyrin dye, and is associated

* Corresponding author. Fax: +81 791 58 0161.
E-mail address: yao@sci.u-hyogo.ac.jp (H. Yao).

1010-6030/$ – see front matter © 2007 Elsevier B.V. All rights reserved.
doi:10.1016/j.jphotochem.2006.12.042

with a different kind of borate anions in the presence of a neutral polymer stabilizer. Well-dispersed TMPyP nanoparticles with narrow size distribution are successfully synthesized, and the optical properties of these nanoparticles are investigated.

2. Experimental

2.1. Chemicals

meso-Tetrakis(1-methylpyridinium-4-yl) porphine (TMPyP; Fig. 1) tetra-*p*-tosylate was purchased from Sigma–Aldrich Chemical Co. and used as received. Polyvinylpyrrolidone (PVP; average M_W = 10,000, Aldrich) was used as a neutral stabilizer to prevent particle agglomeration. Sodium tetraphenylborate (NaTPB, Aldrich), sodium tetrakis(4-fluorophenyl)borate dihydrate (NaTFPB·2H_2O, Aldrich) and sodium tetrakis[3,5-bis(trifluoromethyl)phenyl]borate dihydrate (NaTFMPB·2H_2O, Dojindo Laboratories) were of the highest commercial grade available and used as received without further purification. Chemical structures of these borates are also shown in Fig. 1. These tetrasubstituted borate salts contain hydrophobic bulky anions that are often used for ion-pair extraction [11].

2.2. Synthesis of TMPyP nanoparticles

The porphyrin (TMPyP) nanoparticles were prepared by means of the "ion-association" technique we have developed [10]. A typical preparation procedure was depicted as follows: at room temperature, an appropriate volume of aqueous TMPyP parent solution (0.1 mM) was rapidly added into the aqueous solution containing NaTPB (0.076 mM) and PVP (0.24 mg/mL) under ultrasonication. Further sonication was continued for 10 min. In the reaction, ion association between cationic $TMPyP^{4+}$ and anionic TPB^- provides water-insoluble porphyrin-based nanoparticles. Herein, we call such particles "TMPyP nanoparticles" because their optical properties are dominated by the TMPyP chromophore. The same procedures were performed to synthesize other porphyrin nanoparticles by using TFPB or TFMPB borate anions. For concise, TMPyP nanoparticle samples prepared using TPB, TFPB and TFMPB are referred to as TMPyP-**1**, TMPyP-**2** and TMPyP-**3**, respectively. Note that the increment of PVP concentration caused the formation of similar-sized nanoparticles with ill-contrast images in electron microscopy observations. The final concentrations of TMPyP and TPB (or TFPB, TFMPB) were 0.016 and 0.064 mM, respectively, showing that the net charge ratio of the loaded borate anions to $TMPyP^{4+}$ namely [TPB^-] (or [$TFPB^-$], [$TFMPB^-$])/(4 × [$TMPyP^{4+}$]), was unity (neutral condition). In the nanoparticle preparations, we changed the concentrations of borate anions (or net charge ratios); however, the size and dispersibility did not change. All the experiments were repeated at least three times to check reproducibility.

2.3. Instruments

The morphology and size of TMPyP nanoparticles were observed with a Hitachi S-4800 scanning transmission electron microscope (STEM). A specimen for STEM observations was prepared by dropping the suspension on an amorphous carbon-coated copper mesh. Elemental analyses of C, N, O, F, S and Na were conducted by energy dispersive X-ray (EDX) spectroscopy with an EDAX Genesis-2000 system attached to the S-4800 electron microscope. The measurements of dynamic light scattering (DLS) for nanoparticles in aqueous solution were conducted with an Otsuka ELS-800 electrophoretic light scattering spectrophotometer with a 10 mW He–Ne laser. UV–vis absorption spectra were recorded on a Hitachi U-4100 spectrophotometer. Fluorescence spectra were obtained with a Hitachi F-4500

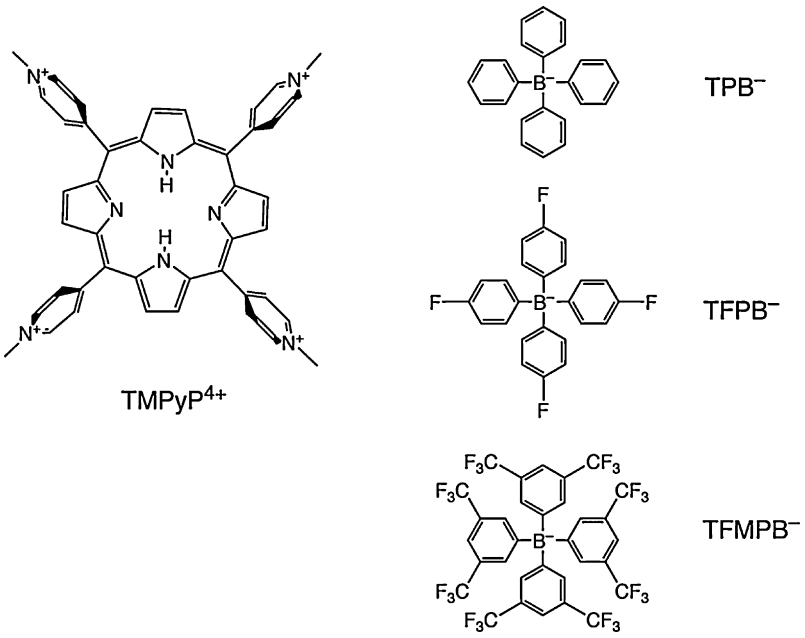

Fig. 1. Chemical structures of TMPyP, TPB, TFPB and TFMPB.

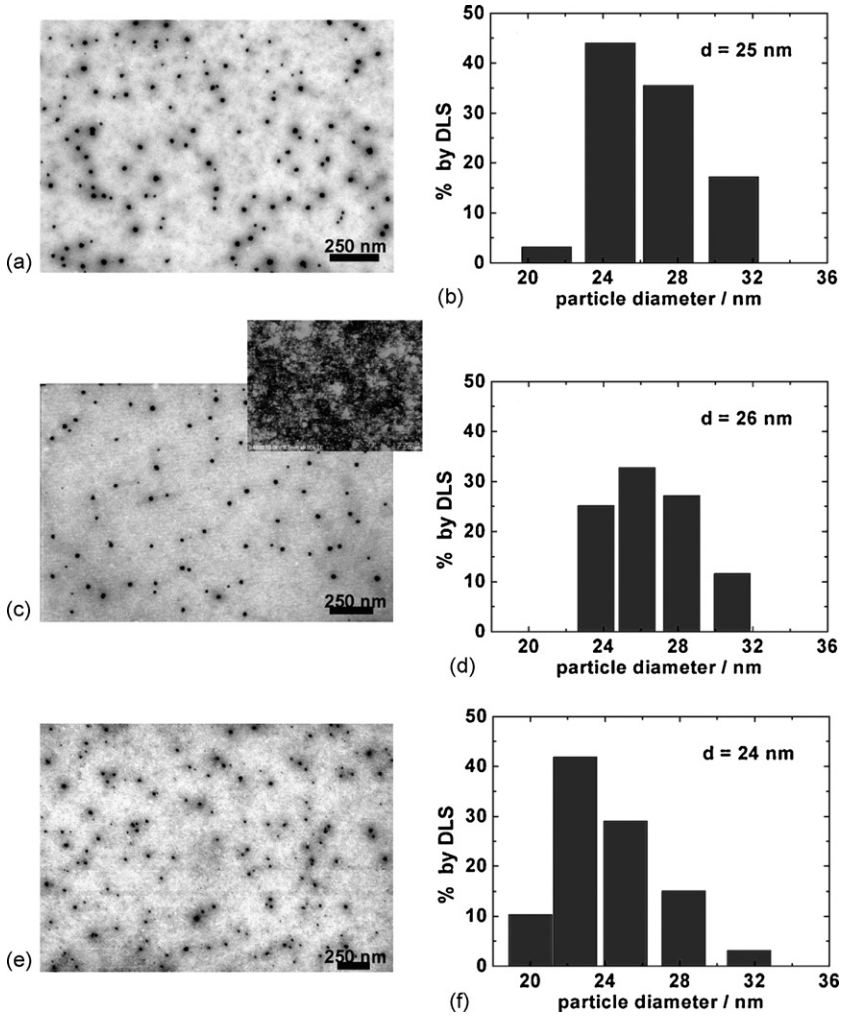

Fig. 2. Left row, STEM images of: (a) TMPyP-**1**, (c) TMPyP-**2** and (e) TMPyP-**3** nanoparticle samples. The inset in (c) shows the sample prepared without using a PVP stabilizer. Right row, size distributions of the corresponding porphyrin nanoparticles of: (b) TMPyP-**1**, (d) TMPyP-**2** and (f) TMPyP-**3** characterized by DLS.

spectrofluorometer. Before the measurements, the samples were freshly prepared and filtered by a 200 nm pore size membrane filter (Sartorious, mini-star RC-15).

3. Results and discussion

3.1. Well-dispersed TMPyP nanoparticles

A series of TMPyP nanoparticles were successfully prepared in aqueous solution.[1] Fig. 2a, c and e shows typical STEM images of porphyrin nanoparticles of TMPyP-**1**, TMPyP-**2** and TMPyP-**3**, respectively. All these samples exhibited a spherical shape with the average diameter of 25 ± 3 nm. From the DLS measurements, the size distribution of each nanoparticle sample could be obtained as shown in Fig. 2b, d or f, suggesting the average diameter of ~24–26 nm and the polydispersity of less than 6%. The diameters estimated by STEM agreed well with those determined by DLS. These TMPyP nanoparticles were stable in solution without precipitation stored under dark at room temperature for at least 30 days. Note that the absence of PVP yielded no stable TMPyP nanoparticles but formed agglomerates (see the inset in Fig. 2c for TMPyP-**2** sample). The agglomeration behavior observed for other two TMPyP nanoparticle samples was similar to that for TMPyP-**2** under the same preparation conditions. Hence, the high dispersion of nanoparticles shown in Fig. 2 indicates that PVP effectively prevents agglomeration of TMPyP nanoparticles by protecting the particle surface in aqueous solution. Crystallographically, the electron diffraction pattern of TMPyP nanoparticles obtained under TEM measurements showed diffusive halos that reveal the amorphous nature of these nanoparticles (see Supplementary data).

The TMPyP nanoparticles are produced via ion-association reaction between $TMPyP^{4+}$ cations and hydrophobic borate anions (TPB^-, $TFPB^-$ or $TFMPB^-$) in the presence of PVP in aqueous solution. In the absence of PVP, the porphyrin nanoparticles were ready to agglomerate with each other (even though the net charge ratio is larger than unity). Furthermore, the average size of TMPyP nanoparticles did not depend on the net

[1] On the basis of the energy dispersive X-ray (EDX) spectral measurements for TMPyP nanoparticles, we have revealed that nanoparticles are composed of an ion-pair complex with TMPyP and each borate used. See Supplementary data for more detail.

charge ratio in the range between 1 and 3. The results indicate that adsorption of excess borate anions (TPB^-, $TFPB^-$ or $TFMPB^-$) onto nanoparticles does not play a sufficient role in stabilizing the nanoparticles. On the basis of the above observations, we can discuss the conceivable mechanism of TMPyP nanoparticle formation: the particle formation process begins with rapid nucleation and formation of small clusters followed by the slow coalescence of these initial clusters into larger particles. In the case of TMPyP nanoparticle formation, a TMPyP cation and a hydrophobic borate anion contact with each other to form an ion-pair complex due to the strong electrostatic attraction [12]. The contact ion-pairs will aggregate themselves by their van der Waals interaction to produce embryos or nuclei, followed by the growth of nuclei into clusters and subsequent larger particles [13]. It is generally accepted that PVP is a common colloid stabilizer for many metal and semiconductor nanoparticles because of its steric effects [14], so this polymer would stabilize the dispersion of organic porphyrin nanoparticles. Probably due to the delicate balance between the promotion and prevention of growth, the similar size distributions of TMPyP-**1**, TMPyP-**2** and TMPyP-**3** samples could be obtained.

3.2. Optical properties of TMPyP nanoparticles

3.2.1. Bathochromic shift of the Soret bands

A series of UV–vis absorption spectra of TMPyP nanoparticles along with the aqueous TMPyP solution (0.01 mM) are shown in Fig. 3. The spectrum of the aqueous TMPyP solution (curve d in Fig. 3) features an intense band around 420 nm known as the Soret band accompanied by four weak Q bands [15,16]. In nanoparticle samples, the Soret band and Q bands exhibit a bathochromic shift compared to those of the aqueous solution. Peak positions of the Soret and Q bands are summarized in Table 1. The changes in the absorption peak positions prove the electrostatic interaction between $TMPyP^{4+}$ and a borate anion (TPB^-, $TFPB^-$ or $TFMPB^-$), resulting in the formation of nanoparticles consisting of TMPyP–borate complexes. Since the sizes of the obtained porphyrin nanoparticles are almost identical with each other, we can conclude that the absorption peak position, especially, the Soret band position, strongly depends on the borate anion used.

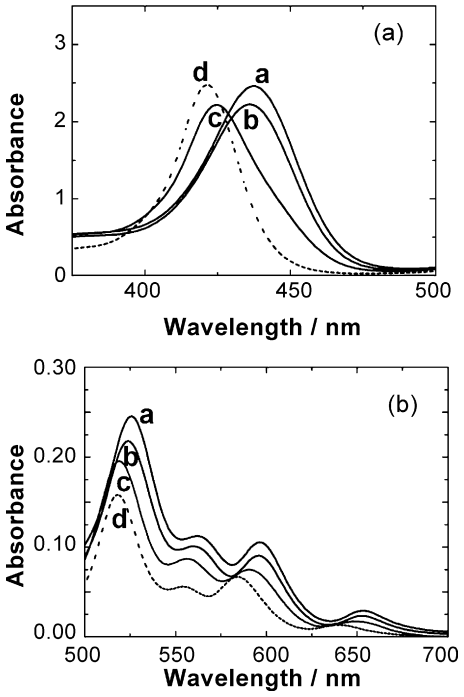

Fig. 3. Absorption spectra in the: (a) Soret band region and the (b) Q band region of TMPyP nanoparticle samples. In each region, curve a, b, c or d shows the spectrum of TMPyP-**1**, TMPyP-**2**, TMPyP-**3** or aqueous TMPyP solution, respectively.

Table 1
Absorption maxima of the Soret and Q bands of TMPyP nanoparticle samples and aqueous TMPyP solution

Samples	Soret band (λ/nm)	Q bands (λ/nm)			
TMPyP-**1**	438	526	562	596	653
TMPyP-**2**	436	524	560	595	652
TMPyP-**3**	425	519	557	590	648
TMPyP	420	518	554	584	638

Regarding the red shift of the Soret band, four explanations have been proposed in the past [4,7,17]: (i) protonation of the porphyrin ring nitrogens, (ii) solvent (or matrix) effect, (iii) aggregation of porphyrin molecules and (iv) flattening of the porphyrin molecule caused by the twisting of four cationic methylpyridinium moieties. In mechanism (i), a highly acidic solution induces the protonation of the porphyrin ring [18]. The pH of the solutions containing the TMPyP nanoparticles were measured to be 7.1–7.3. Because pK_a (at 25 °C) of TMPyP in aqueous solution is reported to be ∼1.3, the protonation mechanism must be ruled out [16]. In addition, the observation of four Q bands for the nanoparticle samples makes this mechanism implausible because diprotonated porphyrins show only two Q bands due to the D_{4h} symmetry of the chromophore [2]. In mechanism (ii), although the absorption band maxima depend on the refractive index of solvents or matrices, very minor spectral shifts of the Soret band (∼2 nm) have been revealed for the TMPyP molecule when the solvents are largely varied [17,19,20]. Thus, this mechanism is also not the main reason of the large red shift of the Soret band.

In mechanism (iii), two types of molecular aggregates involving dipolar coupling are considered with unique electronic and spectroscopic properties: J- and H-type aggregates [21]. When chromophores such as porphyrins are parallel aligned, two new excitonic bands are generated according to a simple exciton theory: one with higher energies and the other with lower than the monomer energy level [21]. In J aggregates, transitions only to the low energy states of the exciton band are allowed. As a consequence, J aggregates exhibit a red-shifted absorption band with respect to the monomer band, and are characterized by almost no Stokes-shifted fluorescence that has a very high quantum yield. In H aggregates, on the other hand, transitions only to the higher level are allowed, yielding a blue shift of the absorption peak. Another consequence of the dipolar coupling in the H aggregate is quenching of fluorescence caused by a rapid internal conversion to the lower energy level and

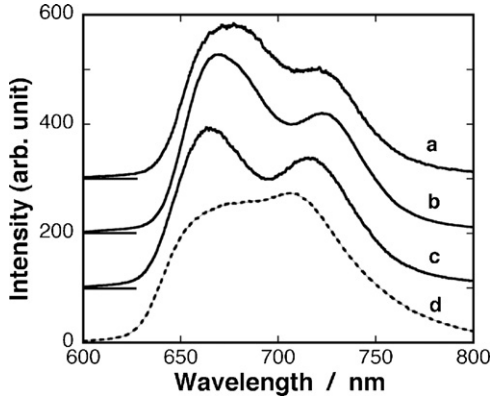

Fig. 4. Fluorescence spectra of: (a) TMPyP-**1**, (b) TMPyP-**2**, (c) TMPyP-**3** and (d) aqueous TMPyP solution. For clarity, the spectra for a–c were offset by adding a constant.

a subsequent forbidden transition to the ground state. Therefore, a shift of the Soret band to longer wavelengths should be attributed to the self-association of porphyrins into J-type aggregates. To confirm whether the porphyrin moieties are self-aggregated or not within the nanoparticles, fluorescence measurements were carried out. Fig. 4 shows typical fluorescence spectra of TMPyP nanoparticles along with that of aqueous TMPyP solution (0.01 mM) excited at 524 nm. Note that the addition of PVP neither quenched the fluorescence of solution-phase TMPyP nor altered its spectral shape. The fluorescence spectra of TMPyP nanoparticles also exhibited a bathochromic shift compared to that of the solution sample, corresponding to the behavior observed in the absorption. In aqueous TMPyP solution [5,15], the Q(0,0) fluorescence band shifts abnormally to a longer wavelength, leading to partial overlap with the Q(0,1) fluorescence band that may be responsible for the ill-resolution of the spectrum. On the other hand, the resolution of the Q(0,0) and Q(0,1) fluorescence bands of TMPyP nanoparticles drastically increased. This issue will be discussed later. A relatively large Stokes shift observed (∼20 nm) confirms the absence of self-aggregation into J aggregates. To discuss more quantitatively, the fluorescence quantum yield (ϕ_f) of these porphyrin nanoparticles was determined. The results are summarized in Table 2 (ϕ_f is in the range of 0.008–0.011) along with the peak positions of the fluorescence bands. The estimated fluorescence quantum yields of the TMPyP nanoparticle systems are quite similar to that of the solution-phase TMPyP,[2] so that J-type self-aggregation does not occur in the nanoparticles. Furthermore, it is reported that the excess addition of H^+TFMPB^- (acid of TFMPB) into organic solvents containing tetra(4-pyridyl)porphine do not bring about the self-aggregation, whereas the addition of HCl or HBr induces aggregation of the porphine itself [22]. This is due to the fact that four sterically demanding anions close to the peripherally cationic porphyrin hinder the further approach of the other porphyrins [22]. These results also strongly support the unaggregated character of TMPyP in a large counteranion (such as TPB^-, $TFPB^-$ or $TFMPB^-$) atmosphere. Therefore, we conclude that TMPyP porphyrin moieties are not self-aggregated within the nanoparticles, and believe this method is highly effective for preparing photofunctional ion-based organic nanoparticles without self-aggregation nor deteriorating the quality of photoluminescence.

The origin of the large red shift of the Soret band is then reasonably attributed to a flattening of the porphyrin molecule (mechanism (iv)). In the molecular structure of TMPyP, the cationic methylpyridinium groups are stable to be almost perpendicular to the plane of the porphine ring [19]. Resonance interaction between the π-system of porphyrin macrocycle and the pyridinium groups then requires a rotation toward a coplanar conformation [15], so the smaller the pyridinium dihedral angle (the orientation of the four pyridinium groups with respect to the porphyrin macrocycle) is, the larger the π-conjugation between the side groups and the porphyrin core becomes [19,20]. Theoretical calculations show that the dihedral angle of ∼60° causes a ∼30 nm red shift in the Soret band of $TMPyP^{4+}$ [19]. Therefore, the large red shift observed in absorption spectra is ascribed to a flattening of the porphyrin molecule in the nanoparticle, that is, the four cationic methylpyridinium moieties are obliquely inclined with respect to the porphyrin ring in the TMPyP nanoparticles. Similar results on the anionic clay–cationic porphyrin complex systems support this interpretation [7].

3.2.2. Counteranion effect

As compared to the Soret band position of aqueous TMPyP solution, nanoparticles show a large red shift in the series of TMPyP-**1** > TMPyP-**2** > TMPyP-**3**. The larger spectral shift means a more enhanced flattening of the porphine molecule

Table 2
Fluorescence properties of various TMPyP nanoparticle samples and aqueous TMPyP solution[a]

Samples	Q (0,0) (λ/nm)	Q (0,1) (λ/nm)	ϕ_f
TMPyP-**1**	677	721	0.008
TMPyP-**2**	671	722	0.011
TMPyP-**3**	663	715	0.010
TMPyP	Not resolved	704	0.011[b]

[a] The spectral shape did not depend on the excitation wavelength. The fluorescence quantum yield of the porphyrin nanoparticles was determined by comparing that of the aqueous TMPyP aqueous solution of $\phi_f = 0.011$ (Ref. [4]; second list). For the estimation, absorbance at λ_{ex} was set to be almost identical and less than 0.1 with each other in all the samples.

[b] Ref. [4]; second list.

[2] One may suppose that the TPB moiety is able to quench the TMPyP fluorescence by electron transfer in the nanoparticles. The oxidation and reduction potentials of $TPB^{0/-}$ and $TMPyP^{4+/3+}$ have been studied in aqueous media and reported to be 1.16 and −0.26 V (versus NHE), respectively. Taking the 0-0 excitation energy of ∼1.85 eV, the Gibbs free energy change (ΔG) of photoinduced electron transfer can be roughly assessed from $\Delta G = 1.16 - (-0.26) - 1.85$ to be −0.43 eV. ((a) Ref. [26]; (b) Ref. [4]; (c) Ref. [27].) Note that the Coulombic term is neglected in the estimation. This value suggests that the electron transfer would be thermodynamically favorable; however, unfavorable rigid conformations or packing between TPB and TMPyP in a solid matrix might restrain the electron transfer process, yielding almost no quenching of TMPyP fluorescence. In the case of TFPB or TFMPB, since the redox potential is reported to be ∼1.5 or ∼3 V (versus NHE), respectively, ΔG increases remarkably (−0.09 or +1.41 eV, respectively), and thus, the electron transfer process will seldom occur energetically. ((a) Ref. [26]; (b) Ref. [28].)

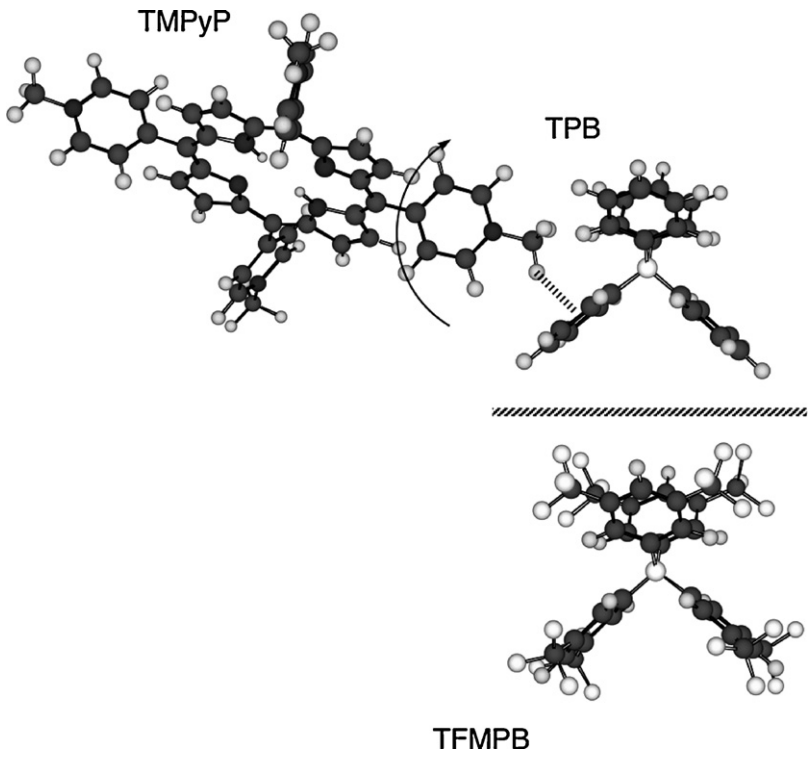

Fig. 5. Schematic illustration of the approach of TPB to the TMPyP molecule. Chemical structure of TFMPB is also shown in the same scale.

including substituent methylpyridinium groups. The fact implies that the steric bulkiness of the borate counteranion strongly correlates with the overall conformation of TMPyP in nanoparticles, that is, with an increase in bulkiness of the borate anion, the flattening of methylpyridinium groups is suppressed. For a relatively small anion such as TPB, it can come closer to the positively charged methylpyridinium groups than a bulky anion such as TFMPB, giving rise to a stronger interaction between the cation and the anion. A schematic illustration of the TPB–TMPyP approach is shown in Fig. 5. The chemical structure of TFMPB is also shown in the same scale. Because of the closer anion approach to the cationic porphyrin, the methylpyridinium substituents can be more rotated such that they occupy smaller void space within the nanoparticle. Using this argument, a difficulty in the close anion approach might allow a conformational relaxation of TMPyP in the nanoparticle, followed by having an intrinsically stable molecular structure of the TMPyP molecule (as can be expected in the TMPyP-**3** nanoparticles).

In addition, discussion through X-ray crystallographic studies for the *N*-methylpyridinium-tetraphenylborate complex will give us some further insight on the interactions between TPB and methylpyridinium moieties in the porphine ring [23]. In the *N*-methylpyridinium–TPB complex, it is known that C–H$\cdots\pi$ interactions contribute to its structural stability. The CH/π interaction is a directional attractive force working between CH groups and π-systems, and plays an important role in stabilizing the structure [24]. Although our porphyrin nanoparticles are not crystalline but amorphous, such CH/π interaction probably also influences the conformations or flattening of methylpyridinium groups of TMPyP in the nanoparticle.

3.2.3. Resolution increase in the fluorescence spectra

At the end, we discuss the increase in the resolution of fluorescence spectra of TMPyP nanoparticles. In the coplanar conformation between the pyridinium groups and porphine ring of TMPyP, strong mixing of the S_1 (singlet excited state) and a close-lying CT (charge transfer from the porphyrin to the pyridinium group) states is expected [15]. Vergeldt et al. estimated the energy of the CT state to be $\sim$2.0 eV, almost equal to the S_1 energy (1.9 eV) [15]. Thus, the mixing of these states results in a featureless or broad fluorescence spectra in aqueous solution (see Fig. 4), that is, an increase in coplanarity of the π-systems caused by the rapid rotation of pyridinium groups upon excitation of TMPyP in water induces a broad fluorescence spectrum.

On the other hand, the CT state of TMPyP is affected by the polarity (or dielectric constant) of a medium [15]. For example, a significant increase of resolution of the Q(0,0) and Q(0,1) bands has been found in methanol because a decrease in the dielectric constant of the solvent destabilizes the CT state of TMPyP, resulting in the reduction of electronic coupling between the unperturbed S_1 and CT states. In consequence, the spectral broadening disappears [15]. Considering that common ionic solids have a relatively low static dielectric constant (for example, 7–8 for calcite and 4.5–4.7 for quartz) [25], the low polarity (or dielectric constant) of the borate solid matrices with abundant phenyl rings is also quite reasonable. In addition, when the TMPyP molecule is immobilized in a solid matrix, rotation of the pyridinium groups toward coplanar geometry is restricted, causing also the reduction of strong mixing of the S_1 and CT states. Hence, the observed spectral resolution increase in the fluorescence of TMPyP nanoparticles is concluded to be caused

by the relatively low matrix polarity and/or immobilization of the pyridinium groups in the solid-state nanoparticles.

4. Conclusions

In the presence of polyvinylpyrrolidone, *meso*-tetrakis(1-methylpyridinium-4-yl) porphine (TMPyP) cations and anionic tetraphenylb orate (TPB) or fluorinated derivatives of TPB reacted with each other in aqueous solution to form ion-pair-based TMPyP nanoparticles. These nanoparticles had well dispersibility and narrow size distribution. No self-aggregation of the constituent porphyrins was observed in the nanoparticle. The absorption spectra of nanoparticles exhibited a large bathochromic shift compared to that of the monomer solution, and the peak position of the Soret band strongly depended on the type of the borate anion used. The flattening of the TMPyP molecules in the nanoparticles, which is caused by the twisting of four cationic methylpyridinium moieties, is the main origin for the large red shift. In the fluorescence properties, a spectral resolution increase could be observed compared to that for the corresponding aqueous-phase porphyrin. We believe that this method provides a useful way to prepare porphyrin nanoparticles under controlled aggregation, and it could be promising for constructing artificial photochemical systems.

Supplementary data

Typical TEM image and the electron diffraction (ED) pattern of TMPyP-**2** nanoparticles, and EDX spectra of the porphyrin nanoparticles.

Appendix A. Supplementary data

Supplementary data associated with this article can be found, in the online version, at doi:10.1016/j.jphotochem.2006.12.042.

References

[1] (a) A. Aviram, M.A. Ratner, Chem. Phys. Lett. 29 (1974) 277;
(b) R.W. Keyes, Phys. Today 45 (1992) 42.

[2] (a) D. Dolphin (Ed.), The Porphyrins, vols. I–VII, Academic Press, New York, 1978;
(b) A. Sane, M.C. Thies, J. Phys. Chem. B 109 (2005) 19688.

[3] (a) S.S. Belanger, J.T. Hupp, Angew. Chem. Int. Ed. 38 (1999) 2222;
(b) P.J. Stang, B. Olenyuk, Acc. Chem. Res. 30 (1997) 502;
(c) R. Rotomskis, R. Augulis, V. Snitka, R. Valiokas, B. Liedberg, J. Phys. Chem. B 108 (2004) 2833;
(d) L.A. Lucia, T. Yui, R. Sasai, S. Takagi, K. Takagi, H. Yoshida, D.G. Whitten, H. Inoue, J. Phys. Chem. B 107 (2003) 3789;
(e) T.J. Marks, Science 227 (1985) 881.

[4] (a) P.M.R. Paulo, S.M.B. Costa, J. Phys. Chem. B 109 (2005) 13928;
(b) K. Kalyanasundaram, M. Neumann-Spallart, J. Phys. Chem. 86 (1982) 5163;
(c) K. Kalyanasundaram, Inorg. Chem. 23 (1984) 2453;
(d) K.M. Kadish, B.G. Maiya, C. Araullo-McAdams, J. Phys. Chem. 95 (1991) 427;
(e) B.P. Neri, G.S. Wilson, Anal. Chem. 44 (1972) 1002;
(f) D.L. Langhus, G.S. Wilson, Anal. Chem. 51 (1979) 1139.

[5] (a) K. Kano, T. Nakajima, S. Hashimoto, J. Phys. Chem. 91 (1987) 6614;
(b) K. Kemnitz, T. Sakaguchi, Chem. Phys. Lett. 196 (1992) 497;
(c) K. Kano, K. Fukuda, H. Wakami, R. Nishiyabu, R.F. Pasternack, J. Am. Chem. Soc. 122 (2000) 7594;
(d) D.L. Akins, H.R. Zhu, C. Guo, J. Phys. Chem. 100 (1996) 5420;
(e) N. Micali, A. Romeo, R. Laucei, R. Purrello, F. Mallamace, L.M. Scolaro, J. Phys. Chem. B 104 (2000) 9416;
(f) R.F. Pasternack, P.R. Huber, P. Boyd, G. Engasser, L. Francesconi, E. Gibbs, P. Fasella, G. Cerio Venturo, L. deC. Hinds, J. Am. Chem. Soc. 94 (1972) 4511;
(g) K. Kano, M. Takei, S. Hashimoto, J. Phys. Chem. 94 (1990) 2181.

[6] (a) R.F. Pasternack, C. Bustamante, P.J. Collings, A. Giannetto, E.J. Gibbs, J. Am. Chem. Soc. 115 (1993) 5393;
(b) M.J. Carvlin, R. Fiel, Nucleic Acids Res. 11 (1983) 6121;
(c) J.M. Kelly, M.J. Murphy, D.J. McConnell, C. OhUigin, Nucleic Acids Res. 13 (1985) 167;
(d) E. Reddi, M. Ceccon, G. Valduga, G. Jori, J.C. Bommer, F. Elisei, L. Latterini, U. Mazzucato, Photochem. Photobiol. 75 (2002) 462;
(e) N.C. Maiti, S. Mazumdar, N. Periasamy, J. Phys. Chem. B 102 (1998) 1528.

[7] (a) M.A. Bos, T.M. Werkhoven, J.M. Kleijn, Langmuir 12 (1996) 3980;
(b) S. Takagi, T. Shimada, M. Eguchi, T. Yui, H. Yoshida, D.A. Tryk, H. Inoue, Langmuir 18 (2002) 2265;
(c) S. Takagi, T. Shimada, T. Yui, H. Inoue, Chem. Lett. (2001) 128;
(d) S. Takagi, D.A. Tryk, H. Inoue, J. Phys. Chem. B 106 (2002) 5455;
(e) Z. Wang, C.J. Medforth, J.A. Shelnutt, J. Am. Chem. Soc. 126 (2004) 15954.

[8] (a) M. Ogawa, K. Kuroda, Chem. Rev. 95 (1995) 399;
(b) K. Takagi, T. Shinchi, Photochem. Rev. 1 (2000) 112.

[9] (a) T. Uemura, S. Kitagawa, J. Am. Chem. Soc. 125 (2003) 7814;
(b) D. Xiao, L. Xi, W. Yang, H. Fu, Z. Shuai, Y. Fang, J. Yao, J. Am. Chem. Soc. 125 (2003) 6740;
(c) X. Gong, T. Milic, C. Xu, J.D. Batteas, C.M. Drain, J. Am. Chem. Soc. 124 (2002) 14290;
(d) T. Sugiyama, T. Asahi, H. Masuhara, Chem. Lett. 33 (2004) 724;
(e) A. Ibanez, S. Maximov, A. Guin, C. Chaillout, P.L. Baldeck, Adv. Mater. 10 (1998) 1540;
(f) H. Kasai, H.S. Nalwa, H. Oikawa, S. Okada, H. Matsuda, N. Minami, A. Kakuta, K. Ono, A. Mukoh, H. Nakanishi, Jpn. J. Appl. Phys. 31 (Part-2) (1992) L1132;
(g) B.K. An, S.K. Kwon, S.D. Jung, S.Y. Park, J. Am. Chem. Soc. 124 (2002) 14410.

[10] (a) H. Yao, Z. Ou, K. Kimura, Chem. Lett. 34 (2005) 1108;
(b) Z. Ou, H. Yao, K. Kimura, Chem. Lett. 35 (2006) 782.

[11] J. Rydberg, M. Cox, C. Musikas, G.R. Choppin, Solvent Extraction Principle and Practice, Marcel Dekker, New York, 2004.

[12] X. Yang, A. Zaitsev, B. Sauerwein, S. Murphy, G.B. Schuster, J. Am. Chem. Soc. 114 (1992) 793.

[13] D. Horn, J. Rieger, Angew. Chem. Int. Ed. 40 (2001) 4330.

[14] (a) R. Si, Y. Zhang, L. You, C. Yan, J. Phys. Chem. B 110 (2006) 5994;
(b) K. Vinodgopal, Y. He, M. Ashokkumar, F. Grieser, J. Phys. Chem. B 110 (2006) 3849;
(c) E. Bekyarova, A. Hashimoto, M. Yudasaka, Y. Hattori, K. Murata, H. Kanoh, D. Kasuya, S. Iijima, K. Kaneko, J. Phys. Chem. B 109 (2005) 3711;
(d) J.I. Paredes, F. Suarez-Garcia, S. Villar-Rodil, A. Martinez-Alonso, J.M.D. Tascon, J. Phys. Chem. B 107 (2003) 8905;
(e) G.W. Busser, J.G. van Ommen, J.A. Lercher, J. Phys. Chem. B 103 (1999) 1651;
(f) L.I. Gabaston, R.A. Jackson, S.P. Armes, Macromolecules 31 (1998) 2883.

[15] F.J. Vergeldt, R.B.M. Koehorst, A. van Hoek, T.J. Schaafsma, J. Phys. Chem. 99 (1995) 4397.

[16] K. Kano, H. Minamizono, T. Kitae, S. Negi, J. Phys. Chem. A 101 (1997) 6118.

[17] (a) L. Ukrainczyk, M. Chibwe, T.L. Pinnavaia, S.A. Boyd, J. Phys. Chem. 98 (1994) 2668;
(b) V.G. Kuykendall, J.K. Thomas, Langmuir 6 (1990) 1350.

[18] S.S. Cady, T.J. Pinnavaia, Inorg. Chem. 17 (1978) 1501.

[19] Z. Chernia, D. Gill, Langmuir 15 (1999) 1625.

[20] I. Renge, J. Phys. Chem. 97 (1993) 6582.
[21] T. Kobayashi (Ed.), J-Aggregates, World Scientific, Singapore, 1996.
[22] G.D. Luca, A. Romeo, L.M. Scolaro, J. Phys. Chem. B 109 (2005) 7149.
[23] S. Kiviniemi, M. Alaviuhkola, K. Rissanen, J. Pursiainen, J. Chem. Soc. Perkin Trans. 2 (2001) 2364.
[24] M. Nishio, M. Hirota, Tetrahedron 45 (1989) 7201.
[25] R.J. Knight, A. Nur, Geophysics 52 (1987) 644.
[26] S.H. Strauss, Chem. Rev. 93 (1993) 927.
[27] K. Lang, P. Kubát, P. Lhoták, J. Mosinger, D.M. Wagnerová, Photochem. Photobiol. 74 (2001) 558.
[28] T. Nagamura, K. Sakai, J. Chem. Soc. Faraday Trans. 1 (84) (1988) 3529.